

Microscopic Interpretation of $K^\pi = 0_2^+, 2_\gamma^+$ Bands in Strongly Deformed Nuclei

A. Georgieva^{1,2}, G. Popa³, and J. P. Draayer²

¹Institute of Nuclear Research and Nuclear Energy,
Bulgarian Academy of Sciences, Sofia 1784, Bulgaria

²Department of Physics and Astronomy, Louisiana State University

³Department of Physics, Rochester Institute of Technology

Abstract.

An overarching $sp(4, R)$ structure is used to identify and link trends in properties of the low-lying, non-yrast states of strongly deformed nuclei. Properties of nuclei within the linked sets are reproduced by using a proton-neutron version of the pseudo- $SU(3)$ shell model.

1 Introduction

An interpretation of the properties of the low-lying spectra of deformed even-even atomic nuclei is usually based first on understanding the structure of states that belong to the ground state band (gsb) and then on properties of the excited bands, including especially the excitation energies of the band-head configurations. While some light nuclei display well-developed rotational characteristics, far and away the majority of nuclei with rotational yrast bands are observed in the heavier shells, that is, among nuclei from the lanthanide and actinide regions. An investigation of the properties of low-lying, non-yrast bands reveals large differences in their behavior. Non-yrast bands of particular interest are those built on the lowest excited $J^\pi = 0^+$ and $K^\pi = 2^+$, $J^\pi = 2^+$ states [1] and are traditionally interpreted as band-heads of the so-called β and γ bands, a labelling that follows from an interpretation of these modes as quadrupole surface vibrations of a deformed liquid drop model [2]. The underlying structures of these bands are described differently depending upon the model one chooses to apply [3]. With the development of new experimental equipment and the accumulation of more data, new model approaches [4] have been introduced in order

to interpret and describe a variety of observed low-lying spectra. There are now many examples against which to test model interpretations of such states. In this report we focus on the first two excited bands which we identify by their band-head quantum numbers $K^\pi = 0_2^+$ and $K^\pi = 2_\gamma^+$.

We give a brief review of the existing data on these bands along with an interpretation of their structure in terms of an $sp(4, R)$ classification scheme, which has been tested empirically and shown to be convenient for a unified description of the low-lying yrast energies of even-even nuclei [5, 6]. As with the previous study, this investigation is aimed at gaining an empirical understanding of the trends in the behavior of these excited bands. Since these low-lying excited non-yrast bands are considerably more complex than the gsb, a deeper investigation into their microscopic structure is required.

To interpret and reproduce properties of the low-lying spectra of deformed even-even nuclei, we apply a proton-neutron version of the pseudo- $SU(3)$ shell model [7]. This scheme is particularly useful since it combines a consideration of the microscopic structure of nuclei with simple but general symmetry principles. Specifically, the pseudo- $SU(3)$ model has been shown to be appropriate for a description of the low-lying spectra of the strongly deformed nuclei [8]. Another advantage of this approach is that it gives a geometrical interpretation of many-nucleon states through an established relationship between the $SU(3)$ invariants and the shape variables β and γ of the Geometrical Collective Model [9].

2 Empirical Investigation and the Classification Scheme

In an empirical investigation of the yrast state energies of deformed nuclei, we achieved an accurate and unified theoretical description by superimposing a classification scheme that linked nuclear species within major valence shell sets [5]. This classification scheme is very convenient because it depends only on two numbers, namely the total number of valence bosons $N = N_\pi + N_\nu$ and the third projection $F_0 = \frac{1}{2}(N_\pi - N_\nu)$ of the F -spin. Equivalently, this is a classification of nuclei in terms of the operators $N_\pi = \frac{1}{2}(N_p - N_p^1)$ and $N_\nu = \frac{1}{2}(N_n - N_n^1)$. These two operators give the number of proton and neutron valence pairs within a given shell beyond their respective closed cores (the usual magic numbers denoted here by N_p^1 and N_n^1) which serve as the vacuum state of the system.

The nuclei belonging to a major nuclear shell, defined by its bordering magic numbers $(N_p^{(1)}, N_n^{(1)} | N_p^{(2)}, N_n^{(2)})$, where $N_p^{(2)} > N_p^{(1)}$ and $N_n^{(2)} > N_n^{(1)}$, are subdivided into two $sp(4, R)$ multiplets determined by whether N is even or odd. The even H_+ (N even) and odd H_- (N odd) spaces of the symplectic algebra [10] are further reduced by an application of the operators N and F_0 to a definite vector within one of these subspaces. Each of the nuclei considered in

this study has a unique N and F_0 value.

As for the case of the empirical investigation of gsb phenomena [5], in the present study we focused on the behavior of the $J^\pi = 0_2^+$ and $J^\pi = 2_\gamma^+$ levels in some F_0 multiplets belonging to different shells. In order to observe some common trends in the variety of structures encountered, we focused on well-deformed nuclei from the lanthanide region [11], specifically considering the behavior of the energies of the $J^\pi = 2^+$ state of the gsb, the first excited $K^\pi = 0_2^+$ state and $K^\pi = 2_\gamma^+$ band-head, in the longest $F_0 = 0$ multiplet of the $(50, 82|82, 126)_+$ shell.

As we can see from Figure 1, the behavior of the 0_2^+ and 2_γ^+ band-head states is strikingly irregular, in contrast with the smooth behavior of the 2^+ energies of the yrast band. This is particularly pronounced in the middle of the shell ($10 < N < 22$), which is a region of well-deformed nuclei, as can be appreciated from the typical $L(L+1)$ rotational spacing of the yrast band states. The gsb $J^\pi = 2^+$ energies for these nuclei lie on an almost straight line at ~ 0.07 MeV. In contrast, the energies of 0_2^+ and 2_γ^+ states oscillate out of phase as a function of N . The trends in the positions of the energies of these states form a pattern that is almost symmetric with respect to the middle of the rotational region at $N = 16$ for ^{164}Dy . At this point, the energy of the first excited $K^\pi = 0^+$ state has its highest value and the band-head of the γ band has its minimum value. To either side of ^{164}Dy for the ^{160}Gd and ^{168}Er we have $E(2_\gamma^+) < E(0_2^+)$. However,

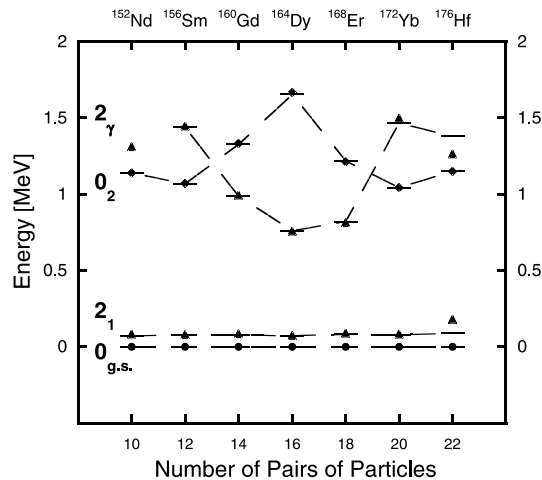


Figure 1. The experimental and theoretical energies of the ground band $J^\pi = 0^+$ and $J^\pi = 2^+$ states and the non-yrast $K^\pi = 0_2^+$ and $K^\pi = 2_\gamma^+$ states of deformed nuclei in the $F_0 = 0$ multiplet of $\text{Sp}(4, \text{R})$. The experimental values are indicated with bars and the calculated numbers with shapes.

away from ^{164}Dy , to the left (^{152}Nd and ^{156}Sm) and to the right (^{172}Yb , ^{176}Hf), the two non-yrast $J^\pi = 0_2^+$ and $K^\pi = 2_\gamma^+$ states change their ordering in energy, $E(2_\gamma^+) > E(0_2^+)$. Three loops are formed by the lines connecting the energies of these states. The first and third loops are quite similar. Our aim is to understand and reproduce this behavior, which has many different model interpretations [1].

3 Outline of the Proton-Neutron Version of the Pseudo- $SU(3)$ Model

The complicated type of behavior noted above is usually strongly dependent upon the microscopic structure of the nucleus [11]. It is well known that the pseudo- $SU(3)$ model is successful in giving a description of the low-energy spectra and electromagnetic transition strengths in heavy deformed nuclei [12]. In contrast to a classification scheme where protons and neutrons pairs are counted as bosons, the proton-neutron version of the pseudo- $SU(3)$ shell model is a fully microscopic theory that respects the Pauli principle.

The model is an extension of the $SU(3)$ shell model [13] for heavy nuclei, and in particular for the lanthanides and actinides where one finds most of the strongly deformed nuclei. In the pseudo- $SU(3)$ version of the model, the pseudo-shell $\tilde{\eta} = \eta - 1$ is defined as the original ‘parent’ shell η without its highest intruder level $j = \eta + \frac{1}{2}$. In the pseudo-shell, containing only the normal parity states, the corresponding pseudo spin-orbit interaction is negligible and hence the $SU(3)$ symmetry is restored. This mapping, from the η to the $\tilde{\eta} = \eta - 1$ shell, yields a symmetry governed reduction of the model space to a subset of $SU(3)$ irreducible representations (irreps) that correspond to the largest intrinsic deformation [14].

The proton and neutron occupancies n_σ ($\sigma = \pi$ and ν , respectively) are determined by filling the Nilsson single-particle levels from below [15] with pairs of particles in each level at a fixed value for the deformation ($\beta \sim 0.3$) for all nuclei. (The changes in predicted occupancies as a function of deformation are rather rare over the normal range of deformation, $\beta \sim 0.25$ to $\beta \sim 0.35$.) Further, we consider only nucleons in normal parity orbits to be spectroscopically active with those in the unique parity orbitals relegated to a renormalization role. This is an assumption that is consistent with what has been done in the past and one that is known to work well for low-lying configurations [16]. Since the nuclei in an $F_0 = 0$ multiplet have an equal number of valence protons and neutrons, the classification number N is equal to the number of valence particles of each kind.

The n_σ^+ nucleons in a normal parity pseudo-shell $\tilde{\eta}_\sigma$ are considered in a ‘strong-coupled’ basis, for which the proton (π) and neutron (ν) pseudo- $SU(3)$ irreps $(\lambda_\sigma, \mu_\sigma)$ are first coupled to a total (λ, μ) with ρ labelling multiple occurrences of the same irrep: $(\lambda_\pi, \mu_\pi) \otimes (\lambda_\nu, \mu_\nu) \rightarrow \rho(\lambda, \mu)$. The quadrupole-

quadrupole ($Q \cdot Q$) interaction is a part of the $SU(3)$ second order operator $C_2 = \frac{1}{4}(Q \cdot Q + 3L^2)$ and gives a dominant weight to the ‘stretched’ coupled representations $(\lambda, \mu) = (\lambda_\pi + \lambda_\nu, \mu_\pi + \mu_\nu)$. However, in order to describe the rich and complex structure of the nuclear spectra, we need to include at least 5 or 6 additional proton and neutron pseudo- $SU(3)$ irreps, which are selected according to their largest C_2 values. A combination of all of these irreps gives a large space of product representations, so they are further truncated in the same way to about 12 or so. The angular momentum quantum number L , with multiplicity label K , is determined through the reduction $SU(3) \supset SO(3)$. The partition of the valence protons and neutrons, into normal ($^+$) and abnormal ($^-$) parity orbits, and the leading pseudo- $SU(3)$ irreps, obtained for the nucleons in the normal parity orbits, are given in Table 1.

Table 1. Occupation numbers for members of the $F_0 = 0$ multiplet.

nucleus	N	n_ν	n_ν^+	n_ν^-	n_π	n_π^+	n_π^-	leading $SU(3)$ irreps		
								(λ, μ)	(λ_π, μ_π)	(λ_ν, μ_ν)
^{152}Nd	10	10	6	4	10	6	4	(30,0)	(12,0)	(18,0)
^{156}Sm	12	12	6	6	12	6	6	(30,0)	(12,0)	(18,0)
^{160}Gd	14	14	8	6	14	8	6	(28,8)	(10,4)	(18,4)
^{164}Dy	16	16	10	6	16	10	6	(30,8)	(10,4)	(20,4)
^{168}Er	18	18	10	8	18	10	8	(30,8)	(10,4)	(20,4)
^{172}Yb	20	20	12	8	20	12	8	(36,0)	(12,0)	(24,0)
^{176}Hf	22	22	12	10	22	12	10	(8,30)	(0,12)	(8,18)

The development of a computer code that enables one to calculate the reduced matrix elements of the physical operators between different $SU(3)$ irreps [17], makes it possible to include interactions that break the $SU(3)$ symmetry. The importance of pairing modes, in the middle of the deformed region, has been pointed out in some studies of $K^\pi = 0^+$ states [18], so these terms are included in our model Hamiltonian. The Hamiltonian, that is appropriate for the description of the nuclei considered, includes spherical single-particle terms for both protons and neutrons, H_{sp}^σ , proton and neutron pairing terms, H_P^σ , an isoscalar quadrupole-quadrupole interaction, $Q \cdot Q$, and four smaller ‘rotor-like’ terms that preserve the pseudo- $SU(3)$ symmetry:

$$H = H_{sp}^\pi + H_{sp}^\nu - G_\pi H_P^\pi - G_\nu H_P^\nu - \frac{1}{2}\chi Q \cdot Q + aJ^2 + bK_J^2 + a_3C_3 + a_{sym}C_2. \quad (1)$$

In the above formula, C_2 and C_3 are the second and third order invariants of $SU(3)$, which are related to the axial and triaxial deformation of the nucleus. In the calculations we assumed fixed values for the proton and neutron

single-particle and pairing interaction strengths, as well as for the quadrupole-quadrupole interaction strength. The strength factor multiplying $Q \cdot Q$ was taken as $35A^{-5/3}$, and the proton and neutron interaction strengths were chosen to be $G_\pi = 21/A$ and $G_\nu = 17/A$ [12]. The pairing force is known to induce K -band mixing and hence deviations from axial symmetry, which in general is favored by the quadrupole-quadrupole interaction [19].

The other interaction strengths were varied to give a best fit for the second $J^\pi = 0^+$, first $J^\pi = 2^+$ and $K^\pi = 2_\gamma^+$ states. The fits were done in the following way: the C_3 interaction strength, a_3 , was varied to fit the energy of the second 0^+ state. The interaction strength b of K_γ^2 was varied to fit the energy of the gamma 2^+ band-head, which is not necessary the second 2^+ state. The interaction strength a of J^2 was varied – but only slightly – to give a best fit to the moment of inertia of the ground state band.

4 Results

A microscopic interpretation of the relative position of a collective band, as well as that of the levels within the band, follows from an evaluation of the primary $SU(3)$ content of the collective state. The latter are closely linked to nuclear deformation. This results from a connection between the microscopic quantum numbers (λ, μ) and the collective shape variables (β, γ) [9].

For ^{160}Gd , ^{164}Dy , and ^{168}Er , in the middle of the shell, the γ band is below the respective $K^\pi = 0_2^+$ band. The ground and γ bands belong to the same $SU(3)$ irrep, when the leading configuration has triaxial character (nonzero $\mu \approx \lambda$). The leading $SU(3)$ irreps, for the three nuclei, have the quantum numbers $\mu > 0$ and $\lambda > \mu$. The gsb and the γ band have similar $SU(3)$ content, and the percentage content of the dominant irrep is always higher in the γ band. There is low content of these irreps in the other bands. The $K^\pi = 0_2^+$ band lies mainly in another $SU(3)$ product configuration. For the ^{164}Dy case, where the band-head of the γ band reaches its highest energy, there is no mixing, that is, the band-head is 100% in the $(10, 4) \otimes (14, 10) \rightarrow (24, 14)$ irrep. Note that this happens also when μ has its largest value.

If the leading $SU(3)$ configuration is prolate ($\mu = 0$), the $K^\pi = 0_2^+$ and $K^\pi = 2^+$ of the γ band come from the same $SU(3)$ irrep. This is the case for both ^{152}Nd and ^{156}Sm at the beginning of the sequence of nuclei that we considered for which $E(2_\gamma^+) > E(0_2^+)$. The ground states are spread over almost all the $SU(3)$ irreps considered in each calculation, with a maximum that is less than 40% in the most symmetric $(12, 0) \otimes (18, 0) \rightarrow (30, 0)$ configuration for ^{156}Sm . The $K^\pi = 0_2^+$ and γ band-heads are also mixed but with about 75% in the coupled $(12, 0) \otimes (12, 6) \rightarrow (24, 6)$ configuration. For ^{152}Nd , a state of angular momentum $J^\pi = 2^+$, $K^\pi = 2^+$ is not known experimentally. As a result of our calculation we predict this state to be at 1.31 MeV within a range of uncertainty that is consistent with others for known states.

At the end of the series, the experimental situation is very similar to the one at the beginning. The ground band for the ^{172}Yb nucleus lies almost 100% in the fully symmetric representation $(36, 0)$ with a very small admixture of $(12, 0) \otimes (16, 10) \rightarrow (28, 10)$, a configuration that plays an important but not dominant role in the γ and $K^\pi = 0_2^+$ band-head configurations. The γ band shows the greatest amount of mixing with the $K^\pi = 0_2^+$ band, with the largest percentage (about 75%) in the triaxial irrep $(4, 10) \otimes (16, 10) \rightarrow (20, 20)$. The L -even states of the $K^\pi = 0_2^+$ and γ bands are almost degenerate. In the case of ^{176}Hf , the protons and neutrons in the normal parity states fill more than half of the shell. Hence the $SU(3)$ quantum numbers for the leading proton $(0, 12)$ and neutron $(8, 18)$ irreps have $\mu > \lambda$, which corresponds to oblate shapes and as a result the pseudo- $SU(3)$ quantum numbers for the leading coupled irrep $(8, 30)$ have also $\lambda < \mu$. In this case, the energy of the $J^\pi = 0_2^+$ state is less than the energy of the $K^\pi = 2^+$ state, as for ^{172}Yb and in the first region, but the $SU(3)$ content in the wave functions is similar to the one in the middle region. The $SU(3)$ content is almost the same in the gsb and $K^\pi = 2_\gamma^+$ state, and this agrees with the picture described in the middle region. The difference is that in this case the energy of $K^\pi = 2_\gamma^+$ state is higher than the one of the first excited 0^+ state, which comes from the respective eigenvalues of the C_3 invariant for these states. This type of nuclei requires further investigation.

Table 2. Interaction strengths of the Hamiltonian.

coef./nucleus	^{152}Nd	^{156}Sm	^{160}Gd	^{164}Dy	^{168}Er	^{172}Yb	^{176}Hf
$a_3 \times 10^{-4}$	2.57	2.59	1.93	0.65	0.75	0.31	0.43
a	0.000	0.000	0.001	-0.001	-0.002	-0.001	-0.007
b	0.00	0.55	0.153	0.042	0.022	0.12	0.3
a_s	0.0000	0.0000	0.0035	0.0008	0.0008	0.001	0.006

The parameters of the Hamiltonian (1) that were obtained through a fitting procedure applied to all of the nuclei considered in this study, are given in Table 2. It is important to note that the pairing interactions split and mix the different $SU(3)$ irreps, and that this mixing introduces triaxiality in the system. The quadrupole-quadrupole interaction drives the proton and neutron systems towards prolate shapes if the oscillator shell is less than half full, towards oblate shapes if the respective shell is more than half full, and to large β values at maximum asymmetry for shells which are roughly half full. In addition to the quadrupole-quadrupole (χ) and the pairing strengths (G_π and G_ν) which change very smoothly as a function of mass, the ‘fine tuning’ of the energies of the nonyrast band states required the use of the other four parameters a_3 , a , b and a_{sym} , which were sufficient determining the correct behavior of the states under consideration and differences in energies of the nuclei with equivalent configurations. The $SU(3)$ configurations that enter into the analysis result from the fact

that the current version of the model focuses only on the particles in the normal parity orbits. The nuclei with the same $SU(3)$ leading irreps (see Table 1) differ by the number of particles in the unique parity states of the Nilsson scheme. With the interaction strengths given in Table 2, the theoretical spectra of the nuclei considered are in good agreement with one another (systematic changes in interaction strengths as a function of mass) and with the experimental data, not only for band-head configurations that we focused on here, but also for the excited states within those bands.

5 Conclusions

In the present application, we achieved a good description of the complex properties of a series of deformed nuclei using a small configuration space. This is a result of the microscopic basis of the model, that correctly takes into account the distribution of particles among the single-particle levels of the valence shell. The combination of proton and neutron valence shells, which are different from one another, are very important in obtaining these results. The coupled pseudo- $SU(3)$ representations that emerge from this analysis, yield information about the deformation of each system. The truncation scheme that is used is also governed by symmetry principles, and tracks the onset of a deformation trough in the coupled representation space. The Hamiltonian of the model includes some terms that are not invariants of $SU(3)$ and therefore split and mix the resultant eigenvectors. In particular, the pairing interactions play a very important role in determining the distribution of the eigenstates across the allowed $SU(3)$ configurations. The four parameters that are used for finely tuning the spectra not only permit a very good reproduction of the experimental data, but also predict the position of states that have not yet been experimentally identified.

Acknowledgments

Support from the U.S. National Science Foundation, PHY-0140300, and the Southeastern Universities Research Association is gratefully acknowledged.

References

- [1] P. E. Garrett (2001) *J. Phys. G: Nucl. Part. Phys.* **27** R1-R22.
- [2] A. Bohr and B. R. Mottelson (1975) *Nuclear Structure*, Vol. II (Benjamin-Cummings, Reading, MA).
- [3] R. K. Sheline (1960) *Rev. of Mod. Phys.* **32** 1.
- [4] F. Iachello and A. Arima (1978) *The Interacting Boson Model* (Cambridge University Press, Cambridge).
- [5] S. Drenska, A. Georgieva, V. Gueorguiev, R. Roussev, and P. Raychev (1995) *Phys. Rev. C* **52** 1853.

- [6] S. Drenska, A. Georgieva, and N. Minkov (2002) *Phys. Rev. C* **65** 054303.
- [7] J. P. Draayer (1993) in *Algebraic Approaches to Nuclear Structure: Interacting Boson and Fermion Models*, Contemporary Concepts in Physics VI, (ed. R. F. Casten; Harwood Academic, Chur, Switzerland) 423.
- [8] J. P. Draayer and K. J. Weeks (1984) *Ann. Phys.* **156** 41.
- [9] Y. Leshber and J. P. Draayer (1987) *Phys. Lett.* **B190** 1; O. Castanos, J. P. Draayer, and Y. Leshber (1988) *Z. Phys. A* **329** 33.
- [10] A. Georgieva, M. Ivanov, P. Raychev, and R. Roussev (1985) *Int. J. Theor. Phys.* **25** 1181.
- [11] D. G. Burke and P. C. Sood (1995) *Phys. Rev. C* **51** 3525.
- [12] G. Popa, J. G. Hirsch, and J. P. Draayer (2000) *Phys. Rev. C* **62** 064313.
- [13] J. P. Elliott (1958) *Proc. R. Soc. London Ser. A* **245** 128; (1958) 562.
- [14] C. Vargas, J. G. Hirsch, P. O. Hess, and J. P. Draayer (1998) *Phys. Rev. C* **58** 1488.
- [15] S. G. Nilsson (1955) *K. Dan. Vidensk. Selsk. Math. Fys. Medd.* **29** No. 16 1.
- [16] J. Escher, J. P. Draayer, and A. Faessler (1995) *Nucl. Phys. A* **586** 73.
- [17] C. Bahri and J. P. Draayer (1994) *Comput. Phys. Commun.* **83** 59.
- [18] O. Mikoshiba, R. Sheline, T. Udagava, and Shiro Yoshida (1967) *Nucl. Phys. A* **101** 202.
- [19] C. Bahri, J. Escher, and J. P. Draayer (1995) *Nucl. Phys. A* **592** 171.